Energy transfer efficiency in the chromophore network strongly coupled to a vibrational mode

Lev G. Mourokh[1,2] and Franco Nori[3,4]
[1]*Department of Physics, Queens College, City University of New York, Flushing, New York 11367, USA*
[2]*Graduate Center of CUNY, New York, New York 10016, USA*
[3]*CEMS, RIKEN, Saitama, 351-0198, Japan*
[4]*Physics Department, University of Michigan, Ann Arbor, Michigan 48109-1040, USA*
(Received 13 July 2014; published 30 November 2015)

Using methods from condensed matter and statistical physics, we examine the transport of excitons through the photosynthetic complex from a receiving antenna to a reaction center. Writing the equations of motion for the exciton creation-annihilation operators, we are able to describe the exciton dynamics, even in the regime when the reorganization energy is of the order of the intrasystem couplings. We determine the exciton transfer efficiency in the presence of a quenching field and protein environment. While the majority of the protein vibrational modes are treated as a heat bath, we address the situation when specific modes are strongly coupled to excitons and examine the effects of these modes on the energy transfer efficiency in the steady-state regime. Using the structural parameters of the Fenna-Matthews-Olson complex, we find that, for vibrational frequencies below 16 meV, the exciton transfer is drastically suppressed. We attribute this effect to the formation of a "mixed exciton-vibrational mode" where the exciton is transferred back and forth between the two pigments with the absorption or emission of vibrational quanta, instead of proceeding to the reaction center. The same effect suppresses the quantum beating at the vibrational frequency of 25 meV. We also show that the efficiency of the energy transfer can be enhanced when the vibrational mode strongly couples to the third pigment only, instead of coupling to the entire system.

DOI: 10.1103/PhysRevE.92.052720 PACS number(s): 87.15.H−, 82.50.−m, 34.50.Ez, 03.65.Yz

I. INTRODUCTION

The effective energy transfer in photosynthetic complexes has been one of the focal points of experimental and theoretical studies over last decades [1–3]. Light energy is absorbed by the pigments in the antenna systems and subsequently transferred to a reaction center, where the created electron-hole pairs are separated and the energy is converted to chemical compounds [4,5]. The process of exciton transfer between the antenna and the reaction center is of special interest, because of the unprecedented transfer efficiency and recent observation of the long-lived quantum coherence in the Fenna-Matthews-Olson (FMO) complex of green sulfur bacteria [6,7] and marine cryptophyte algae [8,9]. The understanding of the energy transfer processes in nature is very important for the development of future artificial light-harvesting devices. Improved engineering could lead to even better energy-transfer efficiency, but various challenges should be first identified and overcome.

The discovery of room-temperature quantum coherence gave rise to extended theoretical studies and to numerous works on the subject [10–28]. Traditional Redfield-type methods assuming a weak coupling of the excitons to protein environment fail for these systems [19,29]. Various approaches have been explored, such as Lindblad [13], small polaron [10,20], numerically-exact quasi-adiabatic propagator path integral [19,21], non-Markovian quantum state diffusion [23], and hierarchical equations of motion [12,30]. Among them, the modified Redfield [31,32] approach demonstrates its effectiveness in the description of the population transfer. However, this method fails to describe the coherent dynamics. This shortcoming has been fixed in the coherent modified Redfield theory (CMRT) [33–35]. In our paper, we use the method of operator equations of motion for the density matrix [36], which is based on the same level of approximations as the CMRT, because it is the most convenient approach for the direct calculation of the energy transfer efficiency.

Exciton transport occurs at elevated temperatures and in the presence of dissipative environment, as well as in various mechanisms of quenching. Nonphotochemical quenching can decrease the energy transfer efficiency, but it can also protect the photosystem in the case of higher than necessary light intensity [37,38]. The effects of the protein environment have been widely discussed. In particular, it was suggested that the interaction with the environment can assist exciton transport [39–46] and, moreover, can lead to a new type of exitonic-vibrational coherence [47–50]. However, it is still an open question how this type of coherence affects the efficiency of the exciton transfer through the chromophore network.

In this paper, we examine the exciton propagation, through a system of many inter-coupled chromophores, to the reaction center, in the presence of an external excitation, radiation heat bath, quenching field, and a protein environment considered as a system of independent oscillators. The main focus here is the coupling to a specific vibrational mode, which cannot be treated as a heat bath. The coupling strengths of all the surrounding components are very different, so various levels of approximations should be used [36]. In particular, the contributions of the quenching and radiation fields, as well as that of the reaction center, are calculated perturbatively within the secular approximation. The reorganization energy of the protein environment is of the order of the interchromophore couplings, so we have to incorporate non-Markovian effects. However, in the case of slow protein motion and high enough temperatures, the dynamics under the time integral can be simplified. We do not apply this approximation for the strongly coupled vibrational mode and also take into account the interplay of the last two processes. For all the above

interactions, we take into account the contributions of both diagonal and off-diagonal elements of the density matrix. The diagonal elements for the vibrational heat bath and for the strongly coupled vibrational mode are treated exactly, whereas the secular approximation is used for the off-diagonal elements [33–36].

The couplings of the system to the external light source and to a reaction center are explicitly included in our Hamiltonian. Therefore, we are able to calculate the rate of energy transfer to the reaction center and the rate of the energy absorbtion by the system and, correspondingly, to *directly* determine the efficiency of the energy transfer. Previously [45,46,51,52], the efficiency was calculated indirectly by the population of the last chromophore in the chain. It should be also emphasized that our approach is not restricted to the single-exciton-propagation case, and the chromophore network can contain as many excitons as the number of chromophores. However, we neglect the exciton annihilation processes [53], which are important for the systems with high exciton density. Including such effects is beyond the scope of our paper and will be addressed in future research.

The couplings of the excitons to a blackbody radiation field and to a quenching field are also explicitly included in the Hamiltonian. The former is responsible for spontaneous electron-hole recombination, while the latter is used to describe nonphotochemical quenching [37,38], represented as an Ohmic external force. It is the competition between this quenching and coupling to the reaction center that determines the efficiency of the energy transfer, and the main goal of our work is to determine how the strong coupling to a vibrational mode affects this competition.

Equations obtained for the general case are applied to the model system having the energetic parameters of the FMO complex but more strongly coupled to the quenching field and to a vibrational mode. This allows us to compare our results with previous studies of this complex. We show that for certain frequencies of the vibrational mode, the energy transfer is strongly suppressed. To explain these results, we determine the time dependencies of the chromophore populations and show that, for these frequencies, the excitation does not effectively reach the chromophore coupled to the reaction center, despite the fact that it has the lowest energy. We argue that this effect is the result of the exitonic-vibrational coherence [47–50], when the *mixed exciton-vibrational mode* is formed and the excitation is transferred between two excitonic states with the emission and absorption of vibrational quanta, instead of proceeding to the reaction center. Eventually the excitation energy is lost to the vibrational heat bath and to the quenching field. The same effect can suppress the quantum beating which occurs in the populations of the first and second pigments. At a certain frequency of the vibrational mode, the mixed exciton-vibrational mode forms between the first and sixth pigments and the exciton is transferred to the sixth chromophore instead of the second one. The inclusion of additional relaxation channels, such as exciton-exciton annihilation, would only suppress the energy transfer even more, further supporting our conclusions. However, if the vibrational mode is strongly coupled to a specific (third) pigment, the efficiency of the energy transfer is even enhanced.

The rest of the paper is structured as follows. Section II contains the Hamiltonian of the system. In Sec. III we determine the density matrix and derive its equations of motion. The efficiency of the energy transfer is defined in Sec. IV. This approach is applied to the FMO complex in Sec. V, where we find the dependence of the energy transfer efficiency on the frequency of the vibrational mode strongly coupled to the system and calculate the time dependencies of the chromophores populations. Section VI contains the conclusions of our work.

II. HAMILTONIAN

We start from the general description of the exciton transfer through a system of N chromophores when these are coupled to each other, and each one of them can be coupled to the light source, reaction center, quenching, and blackbody radiation fields, as well as the protein environment. In addition, the interaction with a specific strong vibrational mode is included. The Hamiltonian of this system consists of the following components:

(1) Unperturbed part:

$$H_0 = \sum_n \epsilon_n a_n^\dagger a_n + \sum_{m\neq n} V_{mn} a_m^\dagger a_n - \sum_n (F_n e^{i\omega_0 t} a_n + F_n^* e^{-i\omega_0 t} a_n^\dagger), \quad (1)$$

where $a_n^\dagger$ and a_n are the creation and annihilation operators for the excitations of the n-th chromophore, respectively, ϵ_n is the excitation energy, V_{mn} is the interchromophores energy transfer amplitude, ω_0 is the frequency of the external light, and F_n is the coupling strengths directly proportional to the dipole moment d_n of the n-chromophore. In this form, the interaction between the chromophore system and the external light is significantly simplified, but it allows us to calculate the absorbed energy and the energy transfer efficiency in a very transparent way. It should be noted that the total number of excitations in the system depends on the coupling to the light source and can be as many as the number of chromophores. However, each of them can only be single populated.

(2) Coupling to the reaction center:

$$H_{\rm trap} = -\sum_n \sum_k (g_{kn} b_k^\dagger a_n + g_{kn}^* a_n^\dagger b_k), \quad (2)$$

where $b_k^\dagger$ and b_k are the creation and annihilation operators, respectively, for the excitations at the reaction center having its own Hamiltonian

$$H_{\rm RC} = \sum_k \epsilon_k b_k^\dagger b_k. \quad (3)$$

(3) Interaction with the blackbody radiation and quenching fields:

$$H_{\rm Rec} = -\sum_n (Q_n a_n^\dagger + Q_n^* a_n), \quad (4)$$

where the operator

$$Q_n = d_n(\mathcal{E}_{\rm rad} + \mathcal{E}_{\rm quen}) \quad (5)$$

is proportional to the sum of the fields multiplied by the dipole moment d_n. The Hamiltonians of the radiation heat bath, $H_{\rm Rad}$, and the quenching field, $H_{\rm quen}$, describe the free evolution of these degrees of freedom.

(4) Coupling to the protein environment:

$$H_{\rm e-ph} = -\sum_{j,n} C_{jn} m_j \omega_j^2 x_j a_n^\dagger a_n. \tag{6}$$

We describe the environment, having the Hamiltonian

$$H_{\rm env} = \sum_j \left(\frac{p_j^2}{2m_j} + \frac{m_j \omega_j^2 x_j^2}{2} \right) \tag{7}$$

as a set of independent harmonic oscillators with the position x_j and momentum p_j operators. The jth oscillator has a mass m_j and a frequency ω_j. Here C_{jn} are the coupling strengths of the jth phonon mode and the exciton at the nth site.

(5) Coupling to a specific vibrational mode:

$$H_{\rm e-vib} = -\sum_n C_n M \Omega^2 X a_n^\dagger a_n \tag{8}$$

with the Hamiltonian

$$H_{\rm vib} = \frac{P^2}{2M} + \frac{M\Omega^2 X^2}{2}, \tag{9}$$

involving the position X and momentum P operators. Here M, Ω, and C_n are the mass, frequency, and the coupling strengths, respectively, associated with this vibrational mode.

The time dependence of the unperturbed Hamiltonian, Eq. (1), can be removed by means of the unitary transformation,

$$U = \exp\left(-i \sum_m N_m \omega_0 t \right) = \prod_m \exp(-i N_m \omega_0 t), \tag{10}$$

where $N_m = a_m^\dagger a_m$. Accordingly, the total Hamiltonian has the form

$$\begin{aligned} H = H_0^U &- \sum_n (e^{i\omega_0 t} Q_n a_n^\dagger + e^{-i\omega_0 t} Q_n^\dagger a_n) \\ &- \sum_{k,n} (e^{-i\omega_0 t} g_{kn} b_k^\dagger a_n + e^{i\omega_0 t} g_{kn}^* a_n^\dagger b_k) \\ &- \sum_{j,n} C_{jn} m_j \omega_j^2 x_j a_n^\dagger a_n - \sum_n C_n M \Omega^2 X a_n^\dagger a_n \\ &+ H_{\rm env} + H_{\rm vib} + H_{\rm RC} + H_{\rm Rad} + H_{\rm quen}, \end{aligned} \tag{11}$$

where

$$\begin{aligned} H_0^U = &\sum_n (\epsilon_n - \omega_0) a_n^\dagger a_n + \sum_{m \neq n} V_{mn} a_m^\dagger a_n \\ &- \sum_n (F_n a_n + F_n^* a_n^\dagger) \end{aligned} \tag{12}$$

is the unperturbed Hamiltonian after the unitary transformation. This transformation allowed us to treat the external light exactly. The obtained Hamiltonian is not purely excitonic, as it includes the ground and excited states mixed by the external light.

III. DENSITY MATRIX AND RATE EQUATIONS

The Hamiltonian, Eq. (12), can be numerically diagonalized, with the determination of its eigenenergies and eigenfunctions, as

$$H_0^U |\mu\rangle = E_\mu |\mu\rangle. \tag{13}$$

Accordingly, we can construct the density matrix in the form

$$\rho_{\mu\nu} = |\mu\rangle\langle\nu| \tag{14}$$

and express all operators in terms of this matrix. In particular, the exciton operators are given by

$$\begin{aligned} a_m &= \sum_{\mu\nu} a_{m;\mu\nu} \rho_{\mu\nu} = \sum_{\mu\nu} \langle\mu|a_m|\nu\rangle \rho_{\mu\nu}, \\ N_m &= a_m^\dagger a_m = \sum_{\mu\nu} \langle\mu|N_m|\nu\rangle \rho_{\mu\nu}. \end{aligned} \tag{15}$$

Correspondingly, the total Hamiltonian of the system can be written as

$$H = H_0^U - \sum_{\mu\nu} \mathcal{A}_{\mu\nu} \rho_{\mu\nu}, \tag{16}$$

where $\mathcal{A}_{\mu\nu}$ includes contributions of all terms of Eq. (11) not involved in H_0. It should be noted that the external light source is already included in H_0 and the basic states are determined accordingly.

It should be noted that our definition of the density matrix [Eq. (14)] is different from the conventionally used one, as it is transposed [36]. However, the mean values determined using these two definitions are identical, and Eq. (14) allows us to treat the density matrix elements $\rho_{\mu\nu}$ as *Heisenberg operators*. The corresponding equations of motion are given by

$$i\dot{\rho}_{\mu\nu} = [\rho_{\mu\nu}, H]_- = -\omega_{\mu\nu}\rho_{\mu\nu} - \sum_\alpha (\mathcal{A}_{\nu\alpha}\rho_{\mu\alpha} - \mathcal{A}_{\alpha\mu}\rho_{\alpha\nu}), \tag{17}$$

where $\omega_{\mu\nu} = E_\mu - E_\nu$.

To evaluate specific contributions to Eq. (17), we apply the approach introduced in Ref. [36], where the set of non-Markovian equations was derived. The coupling strengths of the chromophores to surrounding fields are different, and, correspondingly, various levels of approximations can be used. The details of the calculations are given in the Appendix.

The time evolution of the off-diagonal ($\mu \neq \nu$) elements of the exciton matrix $\langle\rho_{\mu\nu}\rangle(t)$ is given by

$$\begin{aligned} \rho_{\mu\nu}(t) = &\exp[i\omega_{\mu\nu} t] \exp\left[-\left(\bar{\lambda}_{\mu\nu}^{\rm ph} + \bar{\lambda}_{\mu\nu}^{\rm vib} \right) T t^2 \right] \\ &\times \exp[-\Gamma_{\mu\nu} t] \rho_{\mu\nu}(0), \end{aligned} \tag{18}$$

where $\bar{\lambda}_{\mu\nu}^{\rm ph}$ and $\bar{\lambda}_{\mu\nu}^{\rm vib}$ are the reorganization energies associated with the phonon heat bath and the strongly coupled vibrational mode, respectively, and the dephasing rate

$$\Gamma_{\mu\nu} = \Gamma_{\mu\nu}^{\rm ph} + \Gamma_{\mu\nu}^{\rm vib} + \Gamma_{\mu\nu}^{\rm rec} + \Gamma_{\mu\nu}^{\rm trap} \tag{19}$$

includes contributions of all processes involved. It should be emphasized that the exponential factor with the quadratic time dependence is caused by fluctuations of the diagonal elements of the density matrix, which are treated exactly, similar to the modified Redfield approach [31,32] and CMRT [33–35].

The exciton distribution $\langle\rho_\mu\rangle$ over the eigenstates $|\mu\rangle$ of the Hamiltonian H_0 evolves according to the equation

$$\langle\dot{\rho}_\mu\rangle + \gamma_\mu\langle\rho_\mu\rangle = \sum_\alpha \gamma_{\mu\alpha}\langle\rho_\alpha\rangle, \tag{20}$$

where the relaxation matrix $\gamma_{\mu\alpha}$ contains contributions, $\gamma^{\rm ph}_{\mu\alpha}$ and $\gamma^{\rm vib}_{\mu\alpha}$, of the nondiagonal environment and vibrational operators, as well as contributions of recombination, $\gamma^{\rm rec}_{\mu\alpha}$, and trapping, $\gamma^{\rm trap}_{\mu\alpha}$, processes, as

$$\gamma_{\mu\alpha} = \gamma^{\rm ph}_{\mu\alpha} + \gamma^{\rm vib}_{\mu\alpha} + \gamma^{\rm rec}_{\mu\alpha} + \gamma^{\rm trap}_{\mu\alpha}. \tag{21}$$

The density relaxation rate is given by

$$\gamma_\mu = \sum_\alpha \gamma_{\alpha\mu}. \tag{22}$$

The steady-state exciton distribution ρ^0_μ can be found from the equation

$$\gamma_\mu\rho^0_\mu = \sum_\alpha \gamma_{\mu\alpha}\rho^0_\alpha, \tag{23}$$

taking into account the normalization condition $\sum_\mu \rho^0_\mu = 1$.

IV. ENERGY-TRANSFER EFFICIENCY

We define the energy-transfer efficiency as a ratio of the average rate of the energy transmission going to the reaction center to the total rate of electromagnetic energy absorption by the system. The first quantity is given by

$$\mathcal{W}_{\rm RC} = \frac{d}{dt}E_{\rm RC} = \sum_k \epsilon_k\langle\dot{N}_k\rangle, \tag{24}$$

where $N_k = b^\dagger_k b_k$. The interaction of the system with the monochromatic light source can be rewritten in terms of the electric field strength, $\mathcal{E}_n(t) = F_n e^{i\omega_0 t} + {\rm s}$, and the polarization $\mathcal{P}_n = a^\dagger_n + a_n$, as $H_F = -\sum_n \mathcal{E}_n(t)\mathcal{P}_n$. Thus, the rate of the light-energy absorption has the form

$$\mathcal{W} = -\sum_n\langle\mathcal{P}_n\dot{\mathcal{E}}_n(t)\rangle \simeq -i\omega_0\sum_n\langle F_n e^{i\omega_0 t}a_n - F^*_n e^{-i\omega_0 t}a^\dagger_n\rangle. \tag{25}$$

This energy can be determined using the equation of motion for the operator of the total number of excitations, $\sum_m N_m$, and can be written in the form of the balance relation:

$$\mathcal{W} = \mathcal{W}_m + \mathcal{W}_k + \mathcal{W}_{\rm Rec} = \omega_0\sum_m\langle\dot{N}_m\rangle + \omega_0\sum_k\langle\dot{N}_k\rangle + i\omega_0\sum_m\langle e^{-i\omega_0 t}Q^\dagger_m a_m - e^{i\omega_0 t}a^\dagger_m Q_m\rangle. \tag{26}$$

Correspondingly, the energy transfer efficiency is given by

$$\eta = \mathcal{W}_{\rm RC}/\mathcal{W}. \tag{27}$$

For the steady state, the total number of excitons in the system is constant, so $\mathcal{W}_m = 0$. $\mathcal{W}_{\rm RC}$, $\mathcal{W}_k$, and $\mathcal{W}_{\rm Rec}$ can be calculated similar to the relaxation rates of the Appendix, and they have the forms

$$\mathcal{W}_{\rm RC} = \sum_n\sum_{\mu\nu}(\omega_0 - \omega_{\mu\nu})|a_{n;\mu\nu}|^2 \times\left\{\Gamma^{\rm trap}_n(\omega_0 + \omega_{\mu\nu})[1 + n(\omega_0 + \omega_{\mu\nu})]\langle\rho^0_\nu\rangle - \Gamma^{\rm trap}_n(\omega_0 - \omega_{\mu\nu})n(\omega_0 - \omega_{\mu\nu})\langle\rho^0_\mu\rangle\right\}, \tag{28}$$

$$\mathcal{W}_k = \omega_0\sum_n\sum_{\mu\nu}|a_{n;\mu\nu}|^2 \times\left\{\Gamma^{\rm trap}_n(\omega_0 + \omega_{\mu\nu})[1 + n(\omega_0 + \omega_{\mu\nu})]\langle\rho^0_\nu\rangle - \Gamma^{\rm trap}_n(\omega_0 - \omega_{\mu\nu})n(\omega_0 - \omega_{\mu\nu})\langle\rho^0_\mu\rangle\right\}, \tag{29}$$

and

$$\mathcal{W}_{\rm Rec} = 2\omega_0\sum_n\sum_{\mu\nu}|a_{n;\mu\nu}|^2 \times\left\{\chi''_n(\omega_0 + \omega_{\mu\nu})[1 + n(\omega_0 - \omega_{\mu\nu})]\langle\rho^0_\nu\rangle - \chi''_n(\omega_0 - \omega_{\mu\nu})n(\omega_0 - \omega_{\mu\nu})\langle\rho^0_\mu\rangle\right\}. \tag{30}$$

V. FMO COMPLEX

In this section we apply the equations obtained above to a specific system, an FMO complex containing seven pigments. We assume that the external light creates the exciton in the Bchl 1 and the reaction center is coupled to the Bchl 3. Here we ignore the eighth Bchl [54] because its role in the energy transfer is not clear yet. In the absence of an external light source, the energies of the seven exciton sites are given by [55]

$$\begin{aligned}\epsilon_1 &= 1543.18\ {\rm meV},\\ \epsilon_2 &= 1552.48\ {\rm meV},\\ \epsilon_3 &= 1513.42\ {\rm meV},\\ \epsilon_4 &= 1529.54\ {\rm meV},\\ \epsilon_5 &= 1548.76\ {\rm meV},\\ \epsilon_6 &= 1567.36\ {\rm meV},\\ \epsilon_7 &= 1543.8\ {\rm meV}.\end{aligned} \tag{31}$$

The transfer matrix elements (in meV) are [55]

$$V_{mn} = \begin{pmatrix} & -10.87 & 0.68 & -0.73 & 0.83 & -1.7 & -1.23\\ -10.87 & & 3.73 & 1.02 & 0.09 & 1.46 & 0.53\\ 0.68 & 3.73 & & -6.63 & -0.27 & -1.19 & 0.74\\ -0.73 & 1.02 & -6.63 & & -8.77 & -2.11 & -7.85\\ 0.83 & 0.09 & -0.27 & -8.77 & & 10.06 & -0.16\\ -1.7 & 1.46 & -1.19 & -2.11 & 10.06 & & 4.92\\ -1.23 & 0.53 & 0.74 & -7.85 & -0.16 & 4.92 & \end{pmatrix}. \tag{32}$$

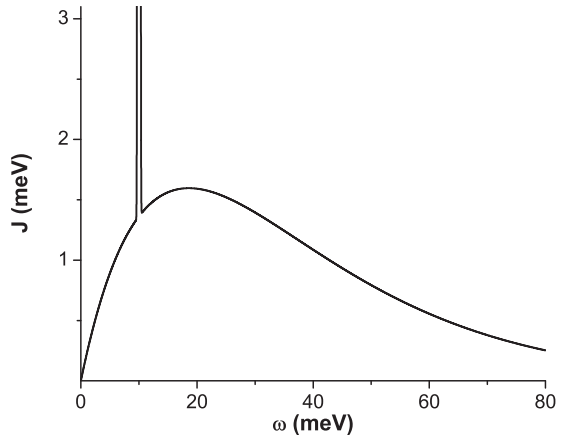

FIG. 1. Environment spectral function $J(\omega)$ including contributions from the heat bath and a specific vibrational mode with frequency $\Omega = 10$ meV.

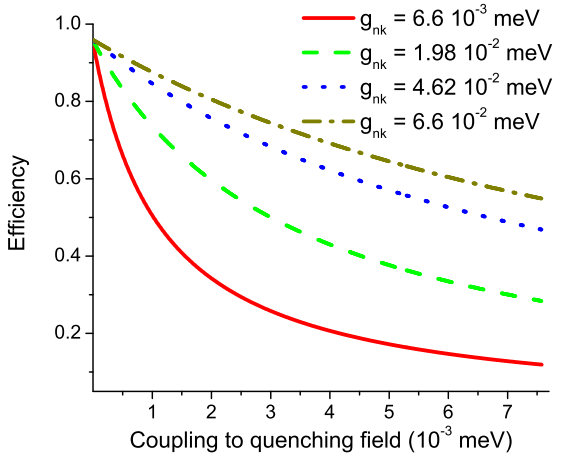

FIG. 2. (Color online) Energy transfer efficiency as a function of the coupling to the quenching field at various couplings to the reaction center.

In our model, each Bchl can be populated, so we have a total of 128 ($= 2^7$) basic states.

To determine the energy transfer efficiency, the spectral functions of the environment should be defined. We use the following form of the spectral function for the heat bath modes:

$$J^{\rm ph}(\omega) = \lambda^{\rm ph}\left(\frac{\omega}{\omega_c}\right)\exp\left(-\frac{\omega}{\omega_c}\right). \tag{33}$$

This type of spectral function is used both for the description of the environment in photosynthetic complexes [56] and for general condensed matter problems [57]. The spectral function for the specific vibrational mode is given by

$$J^{\rm vib}(\omega) = \lambda^{\rm vib}\Omega\,\delta(\omega - \Omega). \tag{34}$$

The total spectral function, including the contributions of the heat bath modes and a specific vibrational mode, is shown in Fig. 1. The cutoff frequency ω_c is taken to be 18.6 meV, and the frequency of the vibrational mode is chosen to be 10 meV for this figure.

The energy of the external light $\hbar\omega_0$ is taken to be 1573.71 meV. This value is resonant to the system of 7 Bchls with energies given by Eq. (31). It should be noted that in the real systems there is always site energy disorder broadening the absorption line of the photosysnthetic complex, but the inclusion of this spectral inhomogeneity into consideration is beyond the scope of our paper.

To determine the parameters used below, we calculate the efficiency [Eq. (27)] for the absence of strong coupling to a specific vibrational mode. The results are shown in Fig. 2, the dependence on the coupling to the quenching field at various values of the coupling to the reaction center, and in Fig. 3, the dependence on the coupling to the reaction center at various values of the coupling to the quenching field. It is evident from these figures that for strong coupling to the reaction center and weak coupling to the quenching field, the efficiency can reach 0.95. To determine the dependence of the energy transfer efficiency on the frequency of the strongly coupled vibrational mode, we choose the coupling to the reaction center $g_{nk} = 6.6 \times 10^{-3}$ meV (with only the third pigment coupled) and the couplings to the quenching field $Q_m = 6.6 \times 10^{-5}, 1.92 \times 10^{-4}$, and 6.6×10^{-4} meV. The other parameters are temperature $T = 77$ K, light-Bchl coupling strength $F = 10^{-4}$ meV (with the light coupled to the first pigment only), refraction index $n_{\rm refr} = 1.42$, heat bath reorganization energy $\lambda^{\rm ph} = 4.34$ meV, and reorganization energy of the vibrational mode $\lambda^{\rm vib} = 18.6$ meV. In this case, the Huang-Rhys factor, defined as the ratio of the reorganization energy and the vibrational frequency, is larger at low frequencies than the experimental values of the FMO complex, which can be up to 0.018 for specific vibrational modes [58]. We would like to emphasize that our model chromophore system has only energetic parameters of the FMO complex but more strongly coupled to the quenching field and to a specific vibrational mode.

The efficiency [Eq. (27)] is shown in Fig. 4 as a function of the frequency of the vibrational mode. One can see that with decreasing frequency, the efficiency starts to drop at approximately 16 meV when the Huang-Rhys factor exceeds one. One can see that this drop can be quite significant, up to four times at low frequencies and moderate coupling to the quenching field.

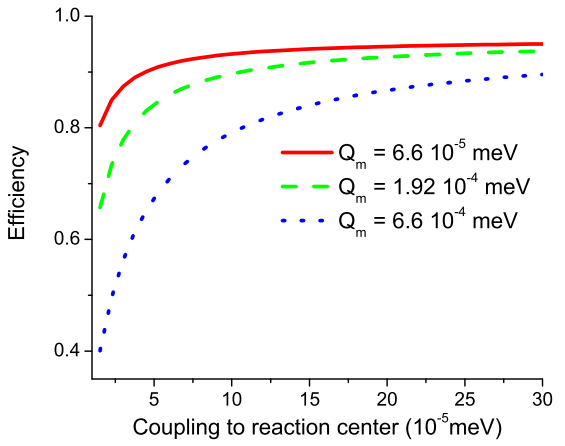

FIG. 3. (Color online) Energy transfer efficiency as a function of the coupling to the reaction center at various couplings to the quenching field.

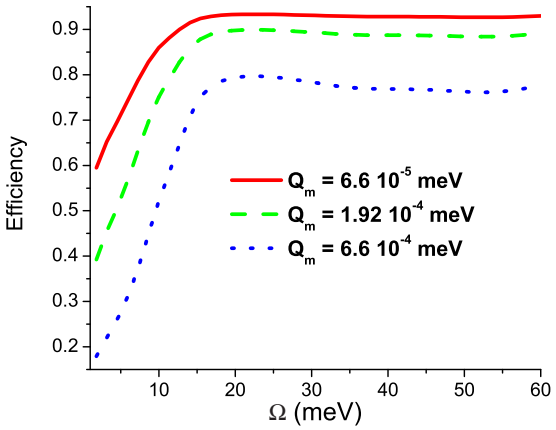

FIG. 4. (Color online) Energy transfer efficiency as a function of the vibrational mode frequency Ω at various couplings to the quenching field.

To understand the physical reasons for such significant drop of the energy transfer efficiency, we calculate the time dependence of the pigment populations with the results shown in Figs. 5(a)–5(f). For initial conditions, we use the situation when the first pigment (coupled to the light) is populated and all other Bchls are not. These initial conditions are quite artificial, but the redistribution of the initial excitation can be shown in a most illuminating way for this case. With no strong coupling to the vibrational mode [Fig. 5(a)], there are well-known quantum oscillations [12] of populations of the first and second pigments (for times of about 0.5 ps), and after about 3 ps the exciton energy is mostly transferred to the third pigment coupled to the reaction center. It should be noted that the fifth, sixth, and seventh pigments remain unpopulated all the time. Almost the same picture can be seen for the high frequency of the vibrational mode [Fig. 5(f)] where the corresponding Huang-Rhys factor is small. With the frequency decreasing, the fifth, sixth, and seventh pigments start to be populated, and at $\Omega = 4$ meV all seven Bchls are populated almost equally by 3 ps. It should be emphasized that the energies of the Bchl 3 and Bchl 4, Bchl 4 and Bchl 5, and Bchl 5 and Bchl 6 are all separated by 16–19 meV. Accordingly, the strong coupling to the vibrational modes of appropriate frequency with the preservation of "vibronic coherence" [47–49] can lead to the formation of "mixed exciton-vibrational modes" between corresponding pigments. Similar phenomenology has been observed in quantum dots [59] where the strong electron-phonon coupling led to a resonant interaction between the discrete (p, 0 LO phonon) state and the continuum of either (s, 1 LO phonon) or (s, 2 LO phonons). As the coupling to the vibrational mode is strong, multiphonon interaction is possible. Formally, it corresponds to nonvanishing contributions of the high-order Bessel functions of Eqs. (A15) and (A16). Moreover, one can see from these equations that the interference between the specific mode and heat bath modes is possible; therefore the energy mismatch preventing the mixed exciton-vibrational mode formation can be compensated by the heat bath. As a result, the exciton, which is transferred to Bchl 3 from Bchl 2, does not proceed to the reaction center, but oscillates between Bchls 3, 4, 5, and 6 and the energy is eventually lost to the quenching field or the heat bath.

Of special interest is the suppression of the quantum beating between Bchl 1 and Bchl 2 at $\Omega = 25$ meV [Fig. 5(e)]. It can be a result of similar mixed exciton-vibrational mode formation. The separation between the energies of Bchl 1 and Bchl 6 is about 24 meV, so vibration-assisted transfer between these

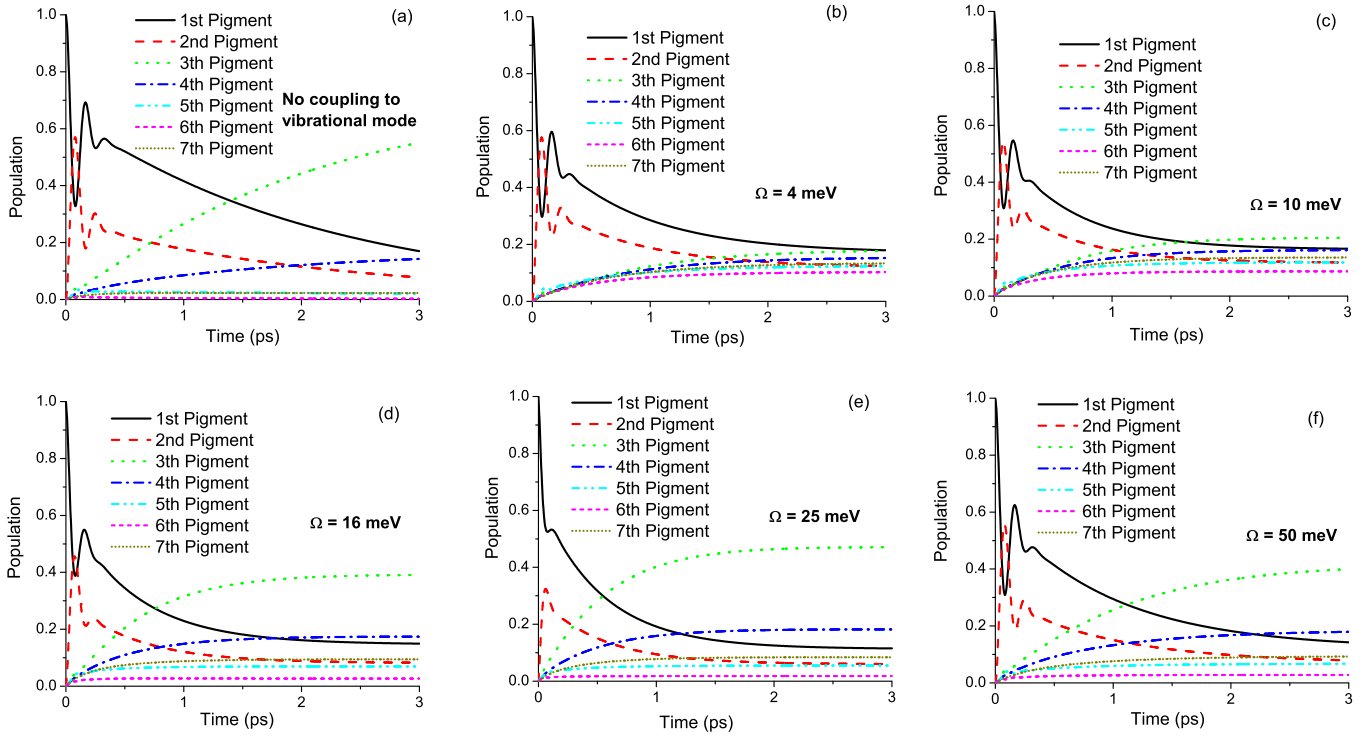

FIG. 5. (Color online) Time dependencies of the pigment populations for various frequencies of the vibrational mode.

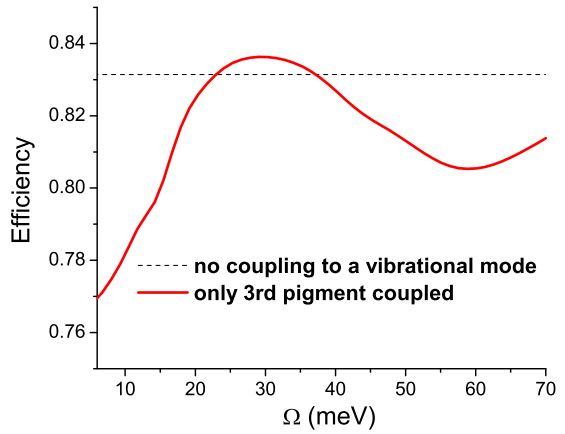

FIG. 6. (Color online) Energy transfer efficiency as a function of the frequency Ω of the vibrational mode coupled only to the third pigment.

pigments is possible. Correspondingly, the exciton proceeds to the third pigment, not via Bchl 2 but via Bchls 6, 5, and 4. It should be noted that the energy efficiency is *not* suppressed at this frequency.

Our approach allows us to examine the situation when the vibrational mode is deliberately coupled to a specific pigment. In Fig. 6 we show the energy transfer efficiency at quite strong coupling to the quenching field, $Q_m = 6.6 \times 10^{-4}$ meV, as a function of the vibrational mode frequency, when only the Bchl 3 is coupled to the vibrational mode. One can see that the efficiency is suppressed at low frequencies but not as drastically as in Fig. 4. The reason for such relatively small suppression is that the mixed exciton-vibrational mode is formed between the Bchl 3 and Bchl 4 only, with no exciton transfer farther to Bchls 5 and 6. However, it is evident from Fig. 6 that at $\Omega = 30$ meV, the energy transfer efficiency even exceeds the value for no coupling to the vibrational mode. The corresponding time dependencies of the pigment populations are shown in Fig. 7. For $\Omega = 4$ meV [Fig. 7(a)], Bchls 5 and 6 remain unpopulated, in contrast to Fig. 5(b), when all the sites are coupled to the vibrational mode. One can see from Fig. 7(b) that for $\Omega = 30$ meV the population of Bchl 3 at 3 ps is even higher than that of the unperturbed system [Fig. 5(a)].

Correspondingly, one can use deliberately coupled vibrations to enhance the efficiency for the case of strong quenching-field coupling.

VI. CONCLUSIONS

In conclusion, we have developed an approach which allows to study the exciton transfer through a network, for the case when the reorganization energy is of the order of the intersite couplings. Our method is not restricted to the one-particle case, so we can describe the propagation of several excitons through the system. We have taken into account the effects of radiative and quenching baths, as well as the coupling to the reaction center, perturbatively using the secular approximation. We have gone beyond this approximation for the protein environment, examining the non-Markovian effects as well. While the majority of the vibrational modes have been treated as a heat bath, we have also included the strong coupling to a specific vibrational mode into consideration. We have used a high-temperature (or low-frequency) approximation for the dynamics inside the non-Markovian integral for the heat bath modes, but not for the strongly coupled vibrational mode. Accordingly, we have determined the contributions of multiphonon processes and obtained that the contributions of the heat bath modes and the vibrational mode are interconnected, as the frequency and the reorganization energy of the vibrational mode is involved in the relaxation matrix for the heat bath and vice versa.

We have obtained the efficiency of the energy transfer directly, as the ratio of the energy transferred to the reaction center and the total energy absorbed by the system. We have calculated this efficiency for a specific system having the structure and the energetic parameters of the FMO complex and strongly coupled to the quenching field and to the vibrational mode and found that this efficiency dropped significantly, if the energy of the strongly coupled vibrational mode becomes smaller than 16 meV. We have attributed that to the formation of "mixed exciton-vibrational modes" where the exciton is transferred back and forth between two pigments with absorption and emission of vibrational quanta. Accordingly, the exciton, instead of proceeding to the reaction center from the lowest-energy Bchl 3, is transferred sequentially to Bchls 4,

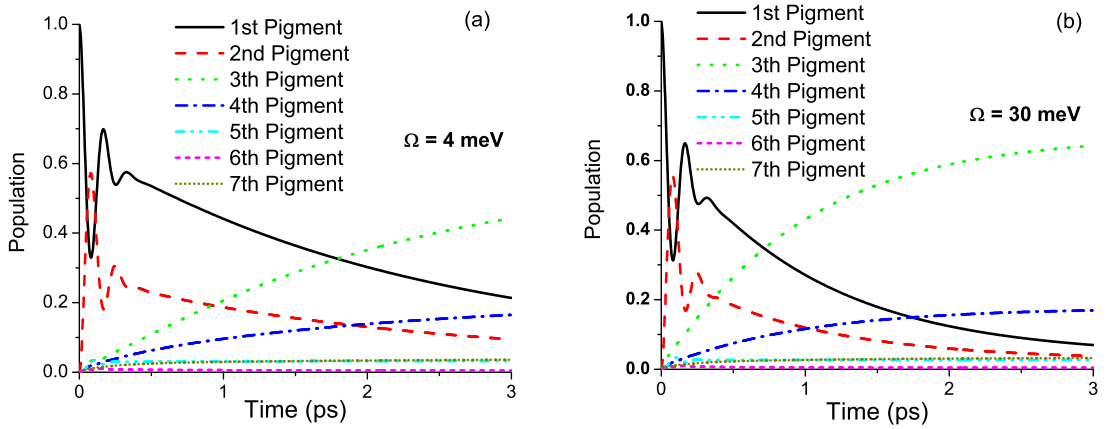

FIG. 7. (Color online) Time dependencies of pigment populations for various frequencies of the vibrational mode coupled only to the third pigment.

5, and 6, and the energy is eventually lost to the quenching field or to the environment heat bath. We have illustrated this effect determining the time dependencies of the pigment populations and showing that for the low frequency of the strongly coupled vibrational mode, the exciton is almost equally distributed between all the pigments. We have obtained the well-known oscillations in the populations of Bchl 1 and Bchl 2 and showed that these oscillations are suppressed at the vibrational mode frequency of 25 meV. This corresponds to the separation of the energies of Bchls 1 and 6, and we attribute this effect to the mixed exciton-vibrational mode between these pigments and the energy transfer avoiding Bchl 2. It is interesting that it does not affect the energy transfer efficiency. We have also shown that the efficiency can even be enhanced if the specific vibrational mode is coupled deliberately to Bchl 3. In this case, the obtained value exceeds that for the unperturbed complex.

ACKNOWLEDGMENTS

The authors are thankful to Dr. Anatoly Smirnov for helpful discussions and to Dr. Neill Lambert for a critical reading of the manuscript. L.M. is partially supported by PSC-CUNY award 65245-00 43. F.N. is partially supported by the RIKEN iTHES Project, the MURI Center for Dynamic Magneto-Optics via the AFOSR award number FA9550-14-1-0040, the IMPACT program of JST, and a Grant-in-Aid for Scientific Research (A).

APPENDIX: CONTRIBUTIONS OF VARIOUS MECHANISMS TO THE EVOLUTION OF THE DENSITY MATRIX

In this Appendix we provide the calculations of various contributions to the equation of motion for the density matrix [Eq. (17)]. The chromophore sites are weakly coupled to the radiative and quenching bath, as well as to the reaction center. Hence, the contribution of these components of the variable $\mathcal{A}$ to Eq. (17) can be treated perturbatively with the secular approximation. Thus, for the diagonal part, $\rho_\mu = \rho_{\mu\mu} = |\mu\rangle\langle\mu|$, of the operator $\rho_{\mu\nu}$ we obtain

$$-i\langle[\rho_\mu, H_{\rm rec} + H_{\rm trap}]_-\rangle = -\sum_\alpha \left(\gamma^{\rm rec}_{\alpha\mu} + \gamma^{\rm trap}_{\alpha\mu}\right)\langle\rho_\mu\rangle + \sum_\alpha \left(\gamma^{\rm rec}_{\mu\alpha} + \gamma^{\rm trap}_{\mu\alpha}\right)\langle\rho_\alpha\rangle. \tag{A1}$$

Recombination events and the trapping of excitations by the reaction center provide the following contribution to the dephasing of excitonic degrees of freedom ($\mu \neq \nu$)

$$-i\langle[\rho_{\mu\nu}, H_{\rm rec} + H_{\rm trap}]_-\rangle = -\left(\Gamma^{\rm rec}_{\mu\nu} + \Gamma^{\rm trap}_{\mu\nu}\right)\langle\rho_{\mu\nu}\rangle. \tag{A2}$$

The relaxation rates are given by

$$\gamma^{\rm rec}_{\mu\alpha} = 2\sum_n |a_{n;\alpha\mu}|^2 \chi''_n(\omega_0 + \omega_{\mu\alpha}) n(\omega_0 + \omega_{\mu\alpha}) + 2\sum_n |a_{n;\mu\alpha}|^2 \chi''_n(\omega_0 - \omega_{\mu\alpha})[1 + n(\omega_0 - \omega_{\mu\alpha})] \tag{A3}$$

and

$$\gamma^{\rm trap}_{\mu\alpha} = \sum_n |a_{n;\alpha\mu}|^2 \Gamma^{\rm trap}_n(\omega_0 + \omega_{\mu\alpha}) n(\omega_0 + \omega_{\mu\alpha}) + \sum_n |a_{n;\mu\alpha}|^2 \Gamma^{\rm trap}_n(\omega_0 - \omega_{\mu\alpha})[1 + n(\omega_0 - \omega_{\mu\alpha})]. \tag{A4}$$

The dephasing rates consist of two parts, $\Gamma^{\rm rec}_{\mu\nu} = \Gamma^{\rm rec}_\mu + \Gamma^{\rm rec}_\nu$, and $\Gamma^{\rm trap}_{\mu\nu} = \Gamma^{\rm trap}_\mu + \Gamma^{\rm trap}_\nu$, where

$$\Gamma^{\rm rec}_\mu = \sum_{n\alpha} |a_{n;\mu\alpha}|^2 \chi''_n(\omega_0 - \omega_{\mu\alpha}) n(\omega_0 - \omega_{\mu\alpha}) + \sum_{n\alpha} |a_{n;\alpha\mu}|^2 \chi''_n(\omega_0 + \omega_{\mu\alpha})[1 + n(\omega_0 + \omega_{\mu\alpha})] \tag{A5}$$

and

$$\Gamma^{\rm trap}_\mu = (1/2)\sum_{n\alpha} |a_{n;\mu\alpha}|^2 \Gamma^{\rm trap}_n(\omega_0 - \omega_{\mu\alpha}) n(\omega_0 - \omega_{\mu\alpha}) + (1/2)\sum_{n\alpha} |a_{n;\alpha\mu}|^2 \Gamma^{\rm trap}_n(\omega_0 + \omega_{\mu\alpha})[1 + n(\omega_0 + \omega_{\mu\alpha})]. \tag{A6}$$

In this expression $n(\omega) = [\exp(\omega/T) - 1]^{-1}$ is the Bose distribution, $\Gamma^{\rm trap}_n$ is the trapping rate defined as

$$\Gamma^{\rm trap}_n = 2\pi \sum_k |g_{kn}|^2 \delta(\omega - \epsilon_k), \tag{A7}$$

and the imaginary part of the bath susceptibility, $\chi''_n(\omega)$, contains contributions of the blackbody heat bath and the Ohmic quenching bath, as

$$\chi''_n(\omega) = (2/3) n_{\rm refr} |d_n|^2 (\omega/c)^3 + \alpha_n \omega, \tag{A8}$$

with $n_{\rm refr}$ being the refractive index of the medium.

The interaction with the protein environment cannot be considered weak, and, correspondingly, we cannot use the perturbative approach employed above. Following Ref. [36], we introduce various spectral densities and reorganization

energies as

$$J_{\mu}^{\rm ph}(\omega)=\sum_j\frac{m_j\omega_j^3}{2}\left(\sum_m C_{jm}\langle\mu|N_m|\mu\rangle\right)^2\delta(\omega-\omega_j),$$

$$\bar{J}_{\mu\nu}^{\rm ph}(\omega)=\sum_j\frac{m_j\omega_j^3}{2}\left(\sum_m C_{jm}\langle\mu|N_m|\mu\rangle-\sum_m C_{jm}\langle\nu|N_m|\nu\rangle\right)^2\delta(\omega-\omega_j),$$

$$\tilde{J}_{\mu\nu}^{\rm ph}(\omega)=\sum_j\frac{m_j\omega_j^3}{2}\left|\sum_m C_{jm}\langle\mu|N_m|\nu\rangle\right|^2\delta(\omega-\omega_j),\quad \mu\neq\nu, \tag{A9}$$

$$\lambda_{\mu}^{\rm ph}=\int_0^\infty\frac{d\omega}{\omega}J_{\mu}^{\rm ph}(\omega)=\sum_j\frac{m_j\omega_j^2}{2}\left(\sum_m C_{jm}\langle\mu|N_m|\mu\rangle\right)^2,$$

$$\bar{\lambda}_{\mu\nu}^{\rm ph}=\int_0^\infty\frac{d\omega}{\omega}\bar{J}_{\mu\nu}^{\rm ph}(\omega)=\sum_j\frac{m_j\omega_j^2}{2}\left(\sum_m C_{jm}\langle\mu|N_m|\mu\rangle-\sum_m C_{jm}\langle\nu|N_m|\nu\rangle\right)^2, \tag{A10}$$

and

$$\lambda_{\mu}^{\rm vib}=\frac{M\Omega^2}{2}\left(\sum_m C_m\langle\mu|N_m|\mu\rangle\right)^2,$$

$$\bar{\lambda}_{\mu\nu}^{\rm vib}=\frac{M\Omega^2}{2}\left(\sum_m C_m\langle\mu|N_m|\mu\rangle-\sum_m C_m\langle\nu|N_m|\nu\rangle\right)^2,$$

$$\tilde{\lambda}_{\mu\nu}^{\rm vib}=\frac{M\Omega^2}{2}\left|\sum_m C_m\langle\mu|N_m|\nu\rangle\right|^2,\quad \mu\neq\nu. \tag{A11}$$

It was shown in Ref. [36] that the contribution of diagonal environmental fluctuations can be determined exactly and they only affect the off-diagonal elements of the density matrix. With inclusion of an additional vibrational mode, the time evolution caused by these diagonal fluctuations has the form

$$\rho_{\mu\nu}(t)=\exp[i\omega_{\mu\nu}t]\exp\left[-\left(\bar{\lambda}_{\mu\nu}^{\rm ph}+\bar{\lambda}_{\mu\nu}^{\rm vib}\right)T\,t^2\right]\rho_{\mu\nu}(0). \tag{A12}$$

We evaluate the internal dynamics in the non-Markovian integrals and obtain the following contributions of the nondiagonal environment and vibrational fluctuations to Eq. (17). (It should be noted that high-temperature and low-environment-frequencies approximations of Ref. [36] have been applied to the heat bath contribution, not to that of the specific single mode.) The evolution of the diagonal matrix elements is given by

$$\langle -i[\rho_\mu,H_{\rm e-ph}+H_{\rm e-vib}]_-\rangle=-\sum_\alpha\left(\gamma_{\alpha\mu}^{\rm ph}+\gamma_{\alpha\mu}^{\rm vib}\right)\langle\rho_\mu\rangle+\sum_\alpha\left(\gamma_{\mu\alpha}^{\rm ph}+\gamma_{\mu\alpha}^{\rm vib}\right)\langle\rho_\alpha\rangle. \tag{A13}$$

For the off-diagonal elements, we obtain

$$\langle -i[\rho_{\mu\nu},H_{\rm e-ph}+H_{\rm e-vib}]_-\rangle=-\left(\Gamma_{\mu\nu}^{\rm ph}+\Gamma_{\mu\nu}^{\rm vib}\right)\langle\rho_{\mu\nu}\rangle. \tag{A14}$$

The relaxation matrices are given by

$$\begin{aligned}\gamma_{\mu\alpha}^{\rm ph}=&\sqrt{\frac{\pi}{\bar{\lambda}_{\alpha\mu}^{\rm ph}T}}\exp\left[-\frac{\bar{\lambda}_{\mu\alpha}^{\rm vib}}{\Omega}\coth\frac{\Omega}{2T}\right]\sum_{l=-\infty}^{\infty}J_l\left[\frac{\bar{\lambda}_{\mu\alpha}^{\rm vib}}{\Omega}\right]\int_0^\infty d\omega\,\tilde{J}_{\alpha\mu}^{\rm ph}(\omega)\,n(\omega)\\
&\times\left[I_0\left(\frac{\bar{\lambda}_{\mu\alpha}^{\rm vib}}{\Omega}\coth\frac{\Omega}{2T}\right)\left\{\exp\left[-\frac{\left(\omega+\Omega_{\alpha\mu}+l\Omega-\bar{\lambda}_{\alpha\mu}^{\rm ph}\right)^2}{4\bar{\lambda}_{\alpha\mu}^{\rm ph}T}\right]+\exp\left(\frac{\omega}{T}\right)\exp\left[-\frac{\left(\omega-\Omega_{\alpha\mu}-l\Omega+\bar{\lambda}_{\alpha\mu}^{\rm ph}\right)^2}{4\bar{\lambda}_{\alpha\mu}^{\rm ph}T}\right]\right\}\right.\\
&+\sum_{s=1}^{\infty}I_s\left[\frac{\bar{\lambda}_{\mu\alpha}^{\rm vib}}{\Omega}\coth\frac{\Omega}{2T}\right]\left(\exp\left[-\frac{\left(\omega+\Omega_{\alpha\mu}+(l+s)\Omega-\bar{\lambda}_{\alpha\mu}^{\rm ph}\right)^2}{4\bar{\lambda}_{\alpha\mu}^{\rm ph}T}\right]+\exp\left[-\frac{\left(\omega+\Omega_{\alpha\mu}+(l-s)\Omega-\bar{\lambda}_{\alpha\mu}^{\rm ph}\right)^2}{4\bar{\lambda}_{\alpha\mu}^{\rm ph}T}\right]\right.\\
&\left.\left.+\exp\left(\frac{\omega}{T}\right)\left\{\exp\left[-\frac{\left(\omega+\Omega_{\alpha\mu}+(l+s)\Omega-\bar{\lambda}_{\alpha\mu}^{\rm ph}\right)^2}{4\bar{\lambda}_{\alpha\mu}^{\rm ph}T}\right]+\exp\left[-\frac{\left(\omega+\Omega_{\alpha\mu}+(l-s)\Omega-\bar{\lambda}_{\alpha\mu}^{\rm ph}\right)^2}{4\bar{\lambda}_{\alpha\mu}^{\rm ph}T}\right]\right\}\right)\right]\end{aligned} \tag{A15}$$

and

$$\gamma_{\mu\alpha}^{\rm vib} = \sqrt{\frac{\pi}{\bar{\lambda}_{\alpha\mu}^{\rm ph} T}} \exp\left[-\frac{\bar{\lambda}_{\mu\alpha}^{\rm vib}}{\Omega}\coth\frac{\Omega}{2T}\right] \sum_{l=-\infty}^{\infty} J_l\left[\frac{\bar{\lambda}_{\mu\alpha}^{\rm vib}}{\Omega}\right] \Omega\, \tilde{\lambda}_{\alpha\mu}^{\rm vib}\, n(\Omega) \Bigg[I_0\left(\frac{\bar{\lambda}_{\mu\alpha}^{\rm vib}}{\Omega}\coth\frac{\Omega}{2T}\right) \Bigg\{ \exp\left[-\frac{\left(\Omega+\Omega_{\alpha\mu}+l\Omega-\bar{\lambda}_{\alpha\mu}^{\rm ph}\right)^2}{4\bar{\lambda}_{\alpha\mu}^{\rm ph} T}\right]$$
$$+ \exp\left(\frac{\Omega}{T}\right) \exp\left[-\frac{\left(\Omega-\Omega_{\alpha\mu}-l\Omega+\bar{\lambda}_{\alpha\mu}^{\rm ph}\right)^2}{4\bar{\lambda}_{\alpha\mu}^{\rm ph} T}\right] \Bigg\} + \sum_{s=1}^{\infty} I_s\left[\frac{\bar{\lambda}_{\mu\alpha}^{\rm vib}}{\Omega}\coth\frac{\Omega}{2T}\right] \Bigg(\exp\left[-\frac{\left(\Omega+\Omega_{\alpha\mu}+(l+s)\Omega-\bar{\lambda}_{\alpha\mu}^{\rm ph}\right)^2}{4\bar{\lambda}_{\alpha\mu}^{\rm ph} T}\right]$$
$$+ \exp\left[-\frac{\left(\Omega+\Omega_{\alpha\mu}+(l-s)\Omega-\bar{\lambda}_{\alpha\mu}^{\rm ph}\right)^2}{4\bar{\lambda}_{\alpha\mu}^{\rm ph} T}\right] + \exp\left(\frac{\Omega}{T}\right) \Bigg\{ \exp\left[-\frac{\left(\Omega+\Omega_{\alpha\mu}+(l+s)\Omega-\bar{\lambda}_{\alpha\mu}^{\rm ph}\right)^2}{4\bar{\lambda}_{\alpha\mu}^{\rm ph} T}\right]$$
$$+ \exp\left[-\frac{\left(\Omega+\Omega_{\alpha\mu}+(l-s)\Omega-\bar{\lambda}_{\alpha\mu}^{\rm ph}\right)^2}{4\bar{\lambda}_{\alpha\mu}^{\rm ph} T}\right] \Bigg\} \Bigg) \Bigg], \tag{A16}$$

where

$$\Omega_{\alpha\mu} = \omega_{\alpha\mu} + \bar{\lambda}_{\mu}^{\rm ph} - \bar{\lambda}_{\alpha}^{\rm ph} + \bar{\lambda}_{\mu}^{\rm vib} - \bar{\lambda}_{\alpha}^{\rm vib} \tag{A17}$$

and $J_l(z)$ and $I_s(z)$ are the ordinary and modified Bessel functions, respectively. It should be emphasized that the heat bath and vibrational contributions are interconnected, as the vibrational mode is involved in the expression for $\gamma_{\mu\alpha}^{\rm ph}$ and vice versa. The ratio of the reorganization energy and the vibrational frequency appeared in the arguments of the Bessel functions is the Huang-Rhys factor. When it is small (at large frequencies) the high-order terms would vanish, however for the low-frequency vibrational modes with large Huang-Rhys factor the multiphonon processes would have significant contributions.

Similar to Ref. [36], the dephasing rates can be expressed as

$$\Gamma_{\mu\nu}^{\rm ph,vib} = \Gamma_{\mu}^{\rm ph,vib} + \Gamma_{\nu}^{\rm ph,vib}, \quad \Gamma_{\mu}^{\rm ph,vib} = \frac{1}{2}\sum_{\alpha} \gamma_{\alpha\mu}^{\rm ph,vib}. \tag{A18}$$

[1] T. Pullerits and V. Sundström, Acc. Chem. Res. **29**, 381 (1996).
[2] G. D. Scholes, G. R. Fleming, A. Olaya-Castro, and R. van Grondelle, Nature Chem. **3**, 763 (2011).
[3] N. Lambert, Y. N. Chen, Y. C. Cheng, C. M. Li, G. Y. Chen, and F. Nori, Nature Phys. **9**, 10 (2013).
[4] H. van Amerongen, L. Valkunas, and R. van Grondelle, *Photosynthetic Excitons* (World Scientific, Singapore, 2000).
[5] R. E. Blankenship, *Molecular Mechanisms of Photosynthesis* (Blackwell Scientific Publications, Oxford, UK, 2002).
[6] G. S. Engel, T. R. Calhoun, E. L. Read, T.-K. Ahn, T. Mancal, Y.-C. Cheng, R. E. Blankenship, and G. R. Fleming, Nature (London) **446**, 782 (2007).
[7] G. Panitchayangkoon, D. Hayes, K. A. Fransted, J. R. Caram, E. Harel, J. Wen, R. E. Blankenship, and G. S. Engel, Proc. Natl. Acad. Sci. USA **107**, 12766 (2010).
[8] E. Collini, C. Y. Wong, K. E. Wilk, P. M. C. Curmi, P. Brumer, and G. D. Scholes, Nature (London) **463**, 644 (2010).
[9] C. Y. Wong, R. M. Alvey, D. B. Turner, K. E. Wilk, D. A. Bryant, P. M. G. Curmi, R. J. Silbey, and G. D. Scholes, Nature Chem. **4**, 396 (2012).
[10] S. Jang, Y.-C. Cheng, D. R. Reichman, and J. D. Eaves, J. Chem. Phys. **129**, 101104 (2008).
[11] T. Renger, Photosynth. Res. **102**, 471 (2009).
[12] A. Ishizaki and G. R. Fleming, Proc. Natl. Acad. Sci. USA **106**, 17255 (2009).
[13] B. Palmieri, D. Abramavicius, and S. Mukamel, J. Chem. Phys. **130**, 204512 (2009).
[14] J. Cao and R. J. Silbey, J. Phys. Chem. A **113**, 13825 (2009).
[15] A. Ishizaki and G. R. Fleming, New J. Phys. **12**, 055004 (2010).
[16] S. Hoyer, M. Sarovar, and K. B. Whaley, New J. Phys. **12**, 065041 (2010).
[17] F. Fassioli and A. Olaya-Castro, New J. Phys. **12**, 085006 (2010).
[18] J. Wu, F. Liu, Y. Shen, J. Cao, and R. J. Silbey, New J. Phys. **12**, 105012 (2010).
[19] P. Nalbach and M. Thorwart, J. Chem. Phys. **132**, 194111 (2010).
[20] S. Jang, J. Chem. Phys. **135**, 034105 (2011).
[21] P. Nalbach, D. Braun, and M. Thorwart, Phys. Rev. E **84**, 041926 (2011).
[22] P. Nalbach, A. Ishizaki, G. R. Fleming, and M. Thorwart, New J. Phys. **13**, 063040 (2011).
[23] G. Ritschel, J. Roden, W. T. Strunz, and A. Eisfeld, New J. Phys. **13**, 113034 (2011).
[24] C. Olbrich, J. Strümpfer, K. Schulten, and U. Kleinekathöfer, J. Phys. Chem. B **115**, 758 (2011).
[25] C. Olbrich, T. L. C. Jansen, J. Liebers, M. Aghtar, J. Strümpfer, K. Schulten, J. Knoester, and U. Kleinekathöfer, J. Phys. Chem. B **115**, 8609 (2011).
[26] D. P. S. McCutcheon and A. Nazir, J. Chem. Phys. **135**, 114501 (2011).
[27] A. Kolli, A. Nazir, and A. Olaya-Castro, J. Chem. Phys. **135**, 154112 (2011).
[28] R. Alicki and W. Miklaszewski, J. Chem. Phys. **136**, 134103 (2012)
[29] A. Ishizaki and G. R. Fleming, J. Chem. Phys. **130**, 234110 (2009).
[30] C. Kreisbeck, T. Kramer, M. Rodriguez, and B. Hein, J. Chem. Theory Comput. **7**, 2166 (2011).

[31] W. Zhang, T. Meier, V. Chernyak, and S. Mukamel, J. Chem. Phys. **108**, 7763 (1998).
[32] M. Yang and G. R. Fleming, Chem. Phys. **282**, 163 (2002).
[33] Q. Ai, Y.-J. Fan, B.-Y. Jin, and Y.-C. Cheng, New J. Phys. **16**, 053033 (2014).
[34] Y.-H. Hwang-Fu, W. Chen, and Y.-C. Cheng, Chem. Phys. **447**, 46 (2015).
[35] Y. Chang and Y.-C. Cheng, J. Chem. Phys. **142**, 034109 (2015)
[36] P. K. Ghosh, A. Yu. Smirnov, and F. Nori, J. Chem. Phys. **134**, 244103 (2011).
[37] A. V. Ruban, M. P. Johnson, and C. D. P. Duffy, Biochim. Biophys. Acta **1817**, 167 (2012).
[38] C. D. P. Duffy, A. V. Ruban, and L. Valcunas, Phys. Chem. Chem. Phys. **15**, 18752 (2013).
[39] M. B. Plenio and S. F. Huelga, New J. Phys. **10**, 113019 (2008).
[40] M. Mohseni, P. Robentrost, S. Lloyd, and A. Aspuru-Guzik, J. Chem. Phys. **129**, 174106 (2008).
[41] P. Robentrost, M. Mohseni, I. Kassal, S. Lloyd, and A. Aspuru-Guzik, New J. Phys. **11**, 033003 (2009).
[42] J. Roden, G. Schulz, A. Eisfeld, and J. Briggs, J. Chem. Phys. **131**, 044909 (2009).
[43] H. Hossein-Nejad, A. Olaya-Castro, and G. Scholes, J. Chem. Phys. **136**, 024112 (2012).
[44] A. Kolli, E. J. O'Reilly, G. Scholes, and A. Olaya-Castro, J. Chem. Phys. **137**, 174109 (2012).
[45] E. K. Irish, R. Gómez-Bombarelli, and B. W. Lovett, Phys. Rev. A **90**, 012510 (2014).
[46] M. del Rey, A. W. Chin, S. F. Huelga, and M. B. Plenio, J. Phys. Chem. Lett. **4**, 903 (2013).
[47] N. Christensson, H. F. Kauffmann, T. Pullerits, and T. Mančal, J. Phys. Chem. B **116**, 7449 (2012).
[48] T. Mančal, N. Christensson, V. Lukeš, F. Milota, O. Bixner, H. F. Kauffmann, and J. Hauer, J. Phys. Chem. Lett. **3**, 1497 (2012).
[49] A. W. Chin, J. Prior, R. Rosenbach, F. Caycedo-Soler, S. F. Huelga, and M. B. Plenio, Nat. Phys. **9**, 113 (2013).
[50] V. Tiwari, W. K. Peters, and D. M. Jonas, Proc. Natl. Acad. Sci. USA **110**, 1203 (2013).
[51] S. Jesenko and M. Žnidarič, J. Chem. Phys. **138**, 174103 (2013).
[52] B. Witt and F. Mintert, New J. Phys. **15**, 093020 (2013).
[53] B. Brüggemann, J. L. Herek, V. Sundström, T. Pullerits, and V. May, J. Phys. Chem. B. **105**, 11391 (2001).
[54] M. S. Am Busch, F. Müh, M. E. Madjet, and T. Renger, J. Phys. Chem. Lett. **2**, 93 (2011).
[55] J. Adolphs and T. Renger, Biophys. J. **91**, 2778 (2006).
[56] M. Cho, H. M. Vaswani, T. Brixner, J. Stenger, and G. R. Fleming, J. Phys. Chem. B **109**, 10542 (2005).
[57] A. J. Leggett, S. Chakravarty, A. T. Dorsey, M. P. A. Fisher, A. Garg, and W. Zwerger, Rev. Mod. Phys. **59**, 1 (1987).
[58] M. Rätsep and A. Freiberg, J. Lumin. **127**, 251 (2007).
[59] S. Hameau, Y. Guldner, O. Verzelen, R. Ferreira, G. Bastard, J. Zeman, A. Lemaitre, and J. M. Gerard, Phys. Rev. Lett. **83**, 4152 (1999).